

Magnetism of 3d transition-metal monolayers on Cu(111) and Ag(111)

P. Krüger

European Synchrotron Radiation Facility, BP 220, 38043 Grenoble, France

M. Taguchi

Abdus Salam ICTP, Condensed Matter Section, P.O. Box 586, 34100 Trieste, Italy

S. Meza-Aguilar

Institut de Physique et de Chimie des Matériaux de Strasbourg, CNRS UMR 7504, 67037 Strasbourg, France

(Received 10 November 1999; revised manuscript received 10 February 2000)

We have studied the magnetism of 3d transition-metal monolayers (ML's) adsorbed on the Cu(111) and Ag(111) substrates by means of *ab initio* electronic structure calculations in several collinear magnetic orders. In comparison with the ML's on Cu(100) and Ag(100), we find many similarities but also interesting differences. The Ni ML's on Cu (111) and Ag(111) are nonmagnetic in contrast to the Ni ML's on Cu(100) and Ag(100), which are ferromagnetic. The Co and Fe ML's on Cu(111) and Ag(111) are ferromagnetic. The middle-of-the-series elements V, Cr, and Mn, usually present antiferromagnetic nearest-neighbor coupling, which is completely frustrated in a fcc (111) ML (triangular lattice). Among the collinear spin structures considered here, we find the following ground states: V/Cu(111) nonmagnetic, V/Ag(111) ferrimagnetic with two up and one down spin in the $\sqrt{3} \times \sqrt{3} R30^\circ$ magnetic unit cell, Cr/Cu(111), Cr/Ag(111), and Mn/Cu(111) row-by-row antiferromagnetic, and Mn/Ag(111) two-rows-by-two-rows antiferromagnetic. We interpret the results in terms of localized spin models and discuss the possibility of more complex, in particular noncollinear magnetic orders. Comparison with inverse photoemission spectroscopy experiments for V and Mn ML's on Ag(111) yields reasonable agreement.

I. INTRODUCTION

In the last decade, magnetic properties of ultrathin transition-metal (TM) films have been a subject of intense research activity. The issues are both fundamental and technological: the effects of reduced dimensionality on itinerant magnetism on the one hand and possible applications in magnetic recording devices on the other hand. For the study of spontaneous (in contrast to substrate-induced) two-dimensional itinerant magnetism, the prototype system is a 3d-TM monolayer (ML) adsorbed on a nonmagnetic substrate. Low-index noble metal surfaces, such as Cu(100), Ag(100), and Au(100), have often been used as substrate because they present a high degree of structural perfection and the growth conditions of the TM film can be well controlled. In the monolayer range, various artificial structures could be stabilized on these surfaces: adsorbed and embedded monolayers [e.g., Mn/Ag(100) and Ag/Mn/Ag(100) (Ref. 1)] as well as ordered surface alloys [e.g., MnCu/Cu(100) (Ref. 2)].

Since the magnetic properties of 3d-TM's depend sensitively on the details of atomic structure, it is worthwhile to study TM ML's of different crystallographic orientation in order to reveal the effects from the change of symmetry and coordination number. Square lattice ML's on noble-metal fcc (100) substrates have been studied extensively. Relatively few works, however, have considered triangular ML's on the fcc (111) surfaces, especially as far as *ab initio* calculations are concerned. This is somewhat surprising since one may expect the growth conditions to be equally good for both surface orientations and the stability to be even higher for the

triangular ML's due to their maximal coordination of 6. In this respect, let us mention the work by Shen *et al.*,³ who succeeded in growing isotropic fcc Fe films on Cu(111) up to a thickness of 6 ML's. Fcc Fe films on Cu(100), on the contrary, are tetragonally distorted in this thickness range.

By means of *ab initio* calculations, the magnetism of 3d TM ML's on Cu(100) and Ag(100) has been studied by Blügel and Dederichs.^{4,5} They showed that on Cu(100) the Fe, Co, and Ni ML's are ferromagnetic with moments comparable to the bulk metals, while the Cr and Mn ML's are $c(2 \times 2)$ antiferromagnetic with strongly enhanced moments compared to the bulk. For the ML's on Ag(100), the same spin orderings were obtained but the moments are larger than on Cu(100). The V ML was found antiferromagnetic on Ag(100) and nonmagnetic on Cu(100).

Triangular TM ML's have been studied within *ab initio* calculations for several systems.⁶⁻⁸ However, to our knowledge, only in the work of Ref. 9 on 3d TM ML's on C(0001), nonferromagnetic spin orders were considered, which is crucial for the middle-of-the-row TM elements V, Cr, and Mn. These elements tend towards antiferromagnetic nearest-neighbor coupling, which is completely frustrated on the triangular lattice. Therefore noncollinear spin orders may arise and longer ranged spin couplings become important. The determination of the ground-state spin order may then be a nontrivial problem even in localized spin models (Ising¹⁰ or Heisenberg¹¹ models).

In this paper, we report *ab initio* band-structure calculations for 3d TM ML's on Cu(111) and Ag(111) in several collinear spin structures. In Sec. II we outline the computational method and comment on the choice of the spin struc-

tures. In Sec. III we present the results, make comparison with 3d TM ML's on Cu(100) and Ag(100),^{4,5} and interpret the results as far as possible within localized spin models. In Sec. IV we present calculated inverse photoemission spectra for V and Mn monolayers on Ag(111) and compare them with available experimental data by Drube and Himpsel.¹² In the last section, we draw some conclusions of this work.

II. COMPUTATION

The spin-polarized electronic structure is calculated by means of the tight-binding linear-muffin-tin orbital method in the atomic sphere approximation (ASA).¹³ For the evaluation of the interatomic contribution of the electrostatic potential only the monopole terms are retained (i.e., the Madelung potential). It has been pointed out (see, e.g., Ref. 14) that the dipole terms must be included in order to obtain accurate values for such quantities as the surface energy or potential barrier at the surface. However, for magnetic moments and energies, which are the only quantities we are interested in here, we believe that the dipole corrections are not very important. Indeed, we generally find good agreement with full potential methods. As far as the total-energy is concerned, we only calculate its difference between different magnetic states in a fixed atomic structure. The (spin integrated) charge distribution is little sensitive to the magnetic order. Therefore the electrostatic energy (and any errors to it) should mainly cancel out when the total-energy difference is taken. We have used the generalized gradient approximation (GGA) to density-functional theory with the Langreth-Mehl-Hu¹⁵ exchange-correlation (XC) potential.

The overlayer-surface system is modeled using the repeated slab geometry. We take a seven-layer fcc (111) slab, consisting of five Cu or Ag layers and one TM ML on each side. The slabs are separated by five layers of empty spheres. This is sufficient to prevent interaction between different slabs, which is controlled through vanishing band dispersion in the direction perpendicular to the slab and vanishing charge in the central layer of empty spheres. We have determined the equilibrium lattice constant of fcc Cu (3.59 Å) and fcc Ag (4.04 Å), in good agreement (−1%) with experiment. We used these calculated values for the Cu and Ag slabs. We did not, however, calculate the equilibrium interlayer distance d at the TM-Cu (or TM-Ag) interface, because the ASA is known to yield bad results for energy changes that are related to anisotropic deformations.¹⁶ Instead, we estimated the quantity d on the assumption of approximately constant atomic volume (see the Appendix for details). We thus took $d(\text{TM-Cu})=d_0(\text{Cu})$ and $d(\text{TM-Ag})=d_0(\text{Ag})-15\%$, where d_0 denotes the distance between two (111) layers in the substrate. Magnetic moments and energies of transition metals in the ML range can be quite sensitive to interfacial relaxation for certain systems [e.g., a Co ML on W(110) (Ref. 17)]. This does not seem to be the case here, as we checked by comparing the present results with a preliminary study¹⁸ on V and Cr ML's on Ag(111), where $d(\text{TM-Ag})=d_0(\text{Ag})$ was used. In the latter case, the magnetic moments and energies are somewhat larger than the present values. Yet for both the V and the Cr ML, the order of stability of the different spin structures is the same for both values of d , and the magnetic moments of the most

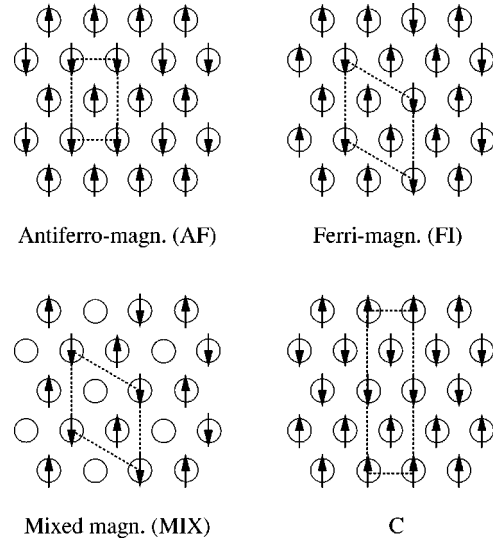


FIG. 1. Scheme of the considered spin structures (other than ferromagnetic). Circles represent transition-metal atoms and arrows indicate the signs of their magnetic moments. Dotted lines delimit the magnetic unit cells.

stable solutions differ by less than 5%.

The k -space integrations were done with the tetrahedron method.¹⁹ We increased the number of k points until the moments were converged to $\pm 0.02\mu_B$ and the magnetic energies to ± 1 meV. Since the different magnetic states have different unit cells and symmetry, it would be misleading to compare the numbers of k points of the irreducible wedges of the different magnetic Brillouin zones (for which the calculations were actually performed). Instead, we refer to the number of k points in the entire first Brillouin zone of the two-dimensional, nonmagnetic, i.e., $p(1\times 1)$ unit cell. We used about 580 such k points for all spin structures.

In order to check the convergence of our results as a function of slab thickness we repeated the calculations for the Fe/Cu system in the ferromagnetic and antiferromagnetic state (see Fig. 1), using an 8-ML-thick Cu(111) film. Compared to the 5-ML Cu(111) film, the magnetic energies were smaller by 3 meV for both ferromagnetic and antiferromagnetic states, while the magnetic moments differed by less than $0.01\mu_B$. Thus we estimate our overall numerical error to less than $0.05\mu_B$ for the moments and less than 5 meV for the magnetic energies.

Choice of spin structures. We are considering the same spin structures as in Ref. 9. Apart from the ferromagnetic state (FO), these are the antiferromagnetic (AF), ferrimagnetic (FI) and mixed-magnetic (MIX) structures depicted in Fig. 1. The choice of these three is motivated by the fact that they represent all possible ground states of the extended Ising model with antiferromagnetic nearest-neighbor (NN) and arbitrary next-nearest-neighbor interaction (NNN) and which includes a repulsive on-site term ($\Delta \sum_i S_i^2, \Delta \geq 0, S_i = 0, \pm 1$). This model was studied by Ballou, Lacroix, and Nunez Regueiro.²⁰ (For $\Delta=0$ and $S_i \neq 0$, the usual Ising model is obtained.) A positive Δ describes a situation where the formation of a magnetic moment is energetically unfavorable, and where a magnetic solution is stabilized by intersite magnetic couplings only. Such a situation may arise close to the magnetic phase transition, and, in case of frus-

TABLE I. Local magnetic moments and magnetic energies per transition-metal atom in the different spin structures (see Fig. 1). In the FI structure, FI+ (FI-) refers to the majority (minority) spins. The moments are absolute values in units of μ_B . The magnetic energies are defined as $E(\text{nonmagnetic}) - E(\text{magnetic})$ and given in units of meV. The exchange coupling constants have been obtained by fitting the relative energies on an Ising model (see text).

| | V | Cr | Mn | Fe | Co | V | Cr | Mn | Fe | Co |
|---|-----------------------|--------|------|------|------|-----------------------|------|------|------|------|
| | Monolayers on Cu(111) | | | | | Monolayers on Ag(111) | | | | |
| Magnetic moments (μ_B , abs. values) | | | | | | | | | | |
| FO | (0.23) | (0.27) | 3.04 | 2.64 | 1.70 | 1.41 | 3.80 | 3.69 | 2.78 | 1.73 |
| AF | | 2.29 | 3.10 | 2.50 | 1.32 | 2.48 | 3.88 | 3.70 | 2.79 | 1.64 |
| FI+ | | 2.06 | 3.22 | 2.49 | 1.46 | 2.37 | 3.97 | 3.69 | 2.68 | 1.66 |
| FI- | | 2.60 | 3.03 | 2.33 | 1.41 | 2.42 | 3.69 | 3.75 | 2.95 | 1.62 |
| MIX | | 2.28 | 2.92 | 2.73 | 1.60 | 2.31 | 3.60 | 3.84 | 2.94 | 1.75 |
| Magnetic energies (meV) | | | | | | | | | | |
| FO | (-2) | (2) | 282 | 544 | 245 | 56 | 573 | 1051 | 808 | 288 |
| AF | | 85 | 478 | 391 | 77 | 172 | 890 | 1071 | 641 | 153 |
| FI | | 57 | 393 | 351 | 98 | 202 | 877 | 1038 | 615 | 163 |
| MIX | | 52 | 227 | 290 | 75 | 118 | 481 | 675 | 485 | 114 |
| Exchange coupling constants (meV) | | | | | | | | | | |
| J_1 | | <0 | -28 | 48 | 37 | <0 | -79 | 3 | 48 | 31 |
| J_2 | | -7 | -21 | -10 | 5 | 7.5 | -3 | -8 | -6.5 | 2.5 |

tration, may lead to mixed magnetic structures.^{20,21}

III. RESULTS AND DISCUSSION

The magnetic moments and energies of all the obtained magnetic solutions are listed in Table I and shown graphically in Figs 2 and 3. From Fig. 2 we see that for a given ML, the modulus of the magnetic moments is roughly independent of the spin order. Exceptions to this rule are the FO states of Cr/Cu(111) and V/Ag(111), which have considerably smaller moments than the other magnetic states. For precisely the same systems, the MIX state is more stable than the FO state, while in all other cases, the MIX state is the least stable magnetic state. This means that for Cr/Cu(111) and V/Ag(111) it is energetically favorable to suppress one-third of the moments such that there are no frustrated (i.e., ferromagnetic) NN couplings left, rather than leaving all NN couplings frustrated. This, as well as the reduced moments in the FO state, indicates that these two systems are antiferromagnets close to the magnetic phase transition. We have

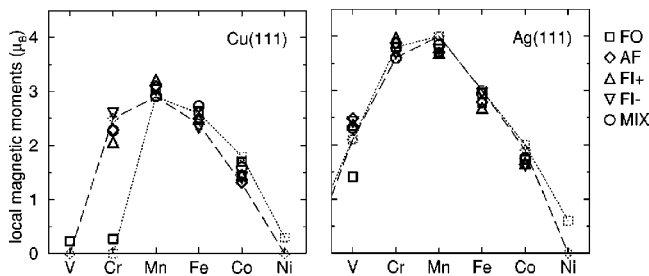


FIG. 2. Symbols in solid lines: local magnetic moments of the different magnetic states (see Fig. 1). This data is identical with that in Table I. The results given in Refs. 4 and 5 for the monolayers on the corresponding (100) substrates are also shown as dotted lines (ferromagnetic state) and broken lines [$c(2 \times 2)$ antiferromagnetic state].

fitted the magnetic energies of the AF, FI, and MIX states onto the extended Ising model with NN and NNN interactions (see Sec. II above). For both Cr/Cu(111) and V/Ag(111), however, we obtain a negative Δ , which is not defined for the extended Ising model. This means that the systems are not close enough to the magnetic transition to be described by this model.

The FO solutions of the V and Cr ML's on Cu(111) have very small magnetic moments and are practically degenerate with the nonmagnetic state (± 2 meV). Their existence is thus very questionable. This is further supported by the fact that these solutions converged to the nonmagnetic state, when we used the local-density approximation (LDA) rather than the GGA (and the corresponding LDA equilibrium lattice constant of Cu, 3.54 Å). We therefore consider them as spurious, which implies that V/Cu(111) is nonmagnetic.

As can be seen in Fig. 3, the Fe and Co ML's have a FO ground state on both substrates. All nonferromagnetic states are much higher in energy. The AF state is lowest in energy

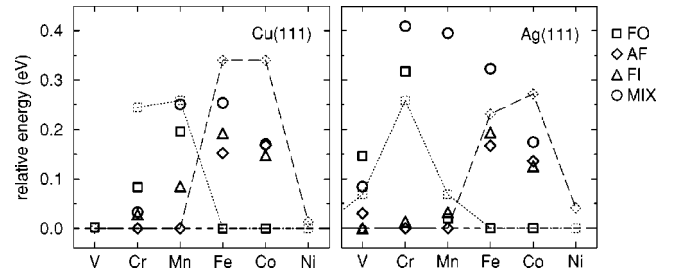


FIG. 3. Symbols in solid lines: relative energies per transition-metal atom of the different magnetic states (see Fig. 1). Except for a change of the origin of the energy scales, the data are the same as that in Table I. The results given in Refs. 4 and 5 for the monolayers on the corresponding (100) substrates are also shown as dotted lines (ferromagnetic state) and broken lines [$c(2 \times 2)$ antiferromagnetic state].

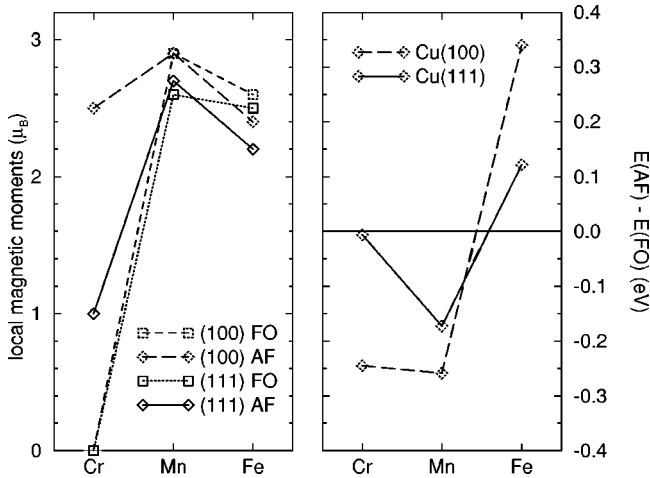


FIG. 4. Magnetic moments and energy difference per transition-metal atom between the ferromagnetic (FO) and antiferromagnetic (AF) states for Cr, Mn, or Fe monolayers on Cu substrates. Comparison between the (100) (from Refs. 4 and 5) and the (111) oriented surfaces. All results in this figure were obtained within the local-density approximation.

for the Mn and Cr ML's on both substrates. For V/Ag(111), the FI state is lowest in energy. However, for V, Cr, Mn on Ag(111), and Cr on Cu(111), the FI-AF energy difference is very small with -30 , 13 , 33 , and 28 meV per TM atom, respectively. Surprisingly, the FO state of Mn/Ag(111) is also only 20 meV per Mn atom above the AF state. While these energy differences are larger than the numerical errors (<5 meV), they are of the same order as other energy scales that are relevant in experiments: the thermal energy at room temperature and possibly that of structural imperfections (monatomic steps, atomic diffusion into the substrate, etc). Therefore comparison with experiment might be difficult in these systems (see also the discussion in Sec. IV).

For comparison, we also show in Figs. 2 and 3 the results of Refs. 4 and 5 for $3d$ TM ML's on Cu(100). Except for Ni, the moments of the (100) ML lie almost on the same line as the (111) ML's and the energy difference between the FO and AF solution follows the same tendencies along the $3d$ series. It must be noted, however, that our results have been obtained within the GGA, while in Refs. 4 and 5 the LDA and slightly different lattice constants were used (3.52 Å for fcc Cu). If we compare (100) and (111) ML's using the same XC potential and the same lattice spacings, we find that the moments and magnetic energies are smaller in the case of the (111) ML's. This can be seen from Fig. 4, where we compared the results of Refs. 4 and 5 for Cr, Mn, and Fe ML on Cu(100) with the corresponding ML's on Cu(111), this time calculated within the LDA (with the Barth-von Hedin²² XC potential) and the corresponding equilibrium lattice constant of 3.54 Å. Considering first Mn and Fe, we see that the moments of the (111) ML's are about 10% smaller and the FO-AF energy difference is only roughly half that of the (100) ML's. In the case of Cr, a FO solution can neither be obtained on Cu(100) nor on Cu(111), but the AF solutions are quite different. While the $c(2 \times 2)$ AF state of the (100) ML is clearly ground state with a magnetic energy of 0.25 eV per atom and a large moment of $2.5\mu_B$, the AF state of the (111) ML is almost degenerate with the nonmagnetic

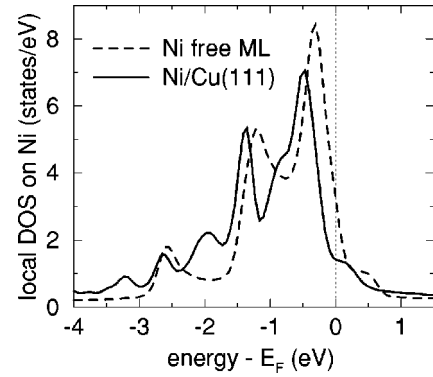


FIG. 5. Local density of states of the nonmagnetic state of a Ni (111) monolayer. Comparison between a monolayer adsorbed on Cu(111) and a free one that has the same lattice constant.

state and its moment is only $1.0\mu_B$. These large differences are a direct consequence of the frustration of the NN antiferromagnetic coupling, as we showed in Ref. 9 for unsupported triangular Cr ML's. Let us note that while the numerical values of the magnetic energies differ considerably between LDA and GGA, the order of stability is the same in all cases that we have checked, including Cr/Cu(111).

Another important difference between the ML's on the (100) surfaces and those on the (111) surfaces is that Ni/Cu(111) and Ni/Ag(111) are nonmagnetic, whereas the Ni/Cu(100) and Ni/Ag(100) are ferromagnetic with moments of 0.3 and $0.6\mu_B$, respectively. For the Cu substrates, this result was already found by Tersoff and Falikov,²³ who used a parametrized tight-binding method. We have also calculated unsupported Ni (111) ML's with the same lattice constant as Ni/Cu(111) and Ni/Ag(111). For both values of the lattice constant, we found a FO ground state with a magnetic moment of $0.8\mu_B$. This means that the vanishing of ferromagnetism in Ni/Cu(111) and Ni/Ag(111) is due to a cooperative effect between the specific electronic structure of a Ni (111) ML and the hybridization with the noble-metal substrate. In Fig. 5 we have compared the local density of states (DOS) of a Ni ML on Cu(111) with that of an unsupported one. In the adsorbed ML, the hybridization with the Cu(111) substrate induces a shift of the high-energy peak to slightly lower energy. This, in turn, causes a decrease of the DOS at the Fermi level by more than a factor of 2, such that the Stoner criterion for ferromagnetism is no longer satisfied.

In order to interpret the energy results in terms of exchange couplings between neighboring atoms, we have fitted the relative energies of the FO, AF, and FI states onto the (normal) Ising model with NN and NNN interactions. The energy is given by $E = -J_1 \sum_1 \sigma_i \sigma_j - J_2 \sum_2 \sigma_i \sigma_j$, where $\sigma_i = \pm 1$ is the spin on site i , the first (second) sum runs over NN (NNN) pairs, and J_1, J_2 are the corresponding coupling constants. We have $J_1 = [E(FI) - E(FO)]/4N$ and $J_2 = [E(AF) - E(FI)]/4N$, where N is the number of sites (i.e., TM atoms). Using the energies from our *ab initio* calculations, we obtain for J_1 and J_2 the values that are listed at the bottom of Table I. Since the FO states of Cr/Cu(111) and V/Ag(111) have much reduced magnetic moments, they should not be used for a fit onto the Ising model, in which the spins have fixed length. Therefore we cannot obtain meaningful values of J_1, J_2 for these two systems. It is obvious,

however, that J_1 is negative (antiferromagnetic NN coupling), since the FO state is clearly less stable than both AF and FI. Note that the J_2/J_1 ratio is very large for the Mn ML's [0.75 for Mn/Cu(111) and -2.7 for Mn/Ag(111)]. This means that the NNN interactions can by no means be neglected. Even more surprisingly, in the case of Mn/Ag(111), the NN coupling is found to be weakly ferromagnetic.

The zero-temperature phase diagram of the Ising model on the triangular lattice with NN and NNN interactions was studied by Tanaka and Uryû.¹⁰ The ground state is: FO for $J_1 > 0, J_2 > -J_1/2$; FI for $J_1 < 0, J_2 > 0$; AF for $J_1 < 0, J_2 < 0$; while for the remaining parameter space, i.e., $J_1 > 0, J_2 < -J_1/2$, it is a two-rows-by-two-rows antiferromagnetic state called "C" in Ref. 10 (see Fig. 1). For all systems except Mn/Ag(111), the Ising model with the parameters in Table I gives the same ground-state spin structure as the *ab initio* calculation. The parameter values of Mn/Ag(111), however, lie in the C phase. For this system, we therefore performed *ab initio* calculations in the spin structure C, too. The magnetic moments are $\mu = \pm 3.65\mu_B$ (Ref. 24) and the magnetic energy is 1082 meV, which is 11 meV higher than that of the AF state. Thus, for a Mn ML on Ag(111), the C state is ground state among the considered magnetic structures as it is expected from the Ising model.

We shall now briefly discuss the possibility of noncollinear magnetic order within the classical Heisenberg (or XY) model, which is the most simple extension of the Ising model that allows for noncollinear spin states. The classical Heisenberg (XY) model is obtained from the Ising model by letting the spins σ_i take on any orientation in three-dimensional (two-dimensional) space. For $J_1 < 0, J_2 = 0$, the ground state is a noncollinear state where any two NN spins form an angle of $2\pi/3$.¹¹ We shall denote it by "120°." It has the same magnetic unit cell as the FI state, and the FI state goes over to the 120° state if one majority spin in the magnetic unit cell is turned by $+\pi/3$ (counterclockwise) and the other one by $-\pi/3$ (clockwise). Considering NN and NNN interactions as before, the 120° state has an energy per site of $3J_1/2 - 3J_2$. This is lower than all Ising model ground states (i.e., FO, AF, FI, and C) if and only if $J_1 < 0, J_2 > J_1/8$. This region covers completely the FI phase and a small part of the AF phase. From the Heisenberg model with the parameters in Table I we therefore expect the 120° state to be ground state for V/Ag(111), Cr/Ag(111), and, if $J_1 < -56$ meV, also for Cr/Cu(111). For simplicity we have restricted our discussion to Ising and Heisenberg models with NN and NNN interactions only. If longer ranged exchange couplings are sufficiently strong, it is clear, however, that various other collinear or noncollinear spin structures may become ground state.²⁵

IV. COMPARISON WITH INVERSE PHOTOEMISSION EXPERIMENTS

Inverse photoemission spectroscopy (IPES) measurements of V and Mn films on Ag(111) in the ML and sub-ML range were reported some time ago by Drube and Himpsel.¹² The experiments were done with normally incident electrons, i.e., the unoccupied electronic states with $k_{\parallel}=0$ were probed. In Figs. 6 and 7 we show the local DOS of Mn and

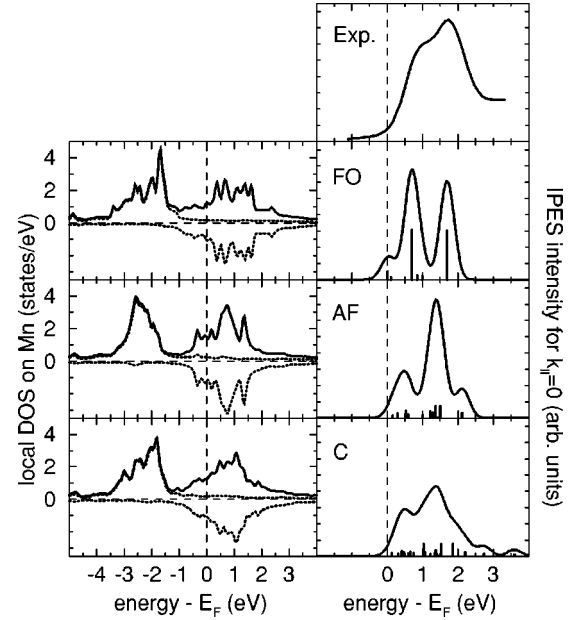


FIG. 6. Mn/Ag(111). Local density of states (DOS) on Mn (left) and the Mn contribution to the inverse photoemission spectra (IPES) for $k_{\parallel}=0$ (right). Comparison between the experimental IPES (Expt.) from Ref. 12 and calculated IPES in different magnetic structures (see Fig. 1). For the calculated IPES Gaussian broadening with 0.47 eV FWHM was used. Solid lines: spin-integrated data. Dotted lines: locally spin-projected DOS.

V ML's on Ag(111) for different magnetic states as well as, for the unoccupied states, the contribution from $k_{\parallel}=0$. The latter can directly be compared with experimental IPES data where the Ag contribution has been subtracted. Such data is also shown in Figs. 6 and 7 (taken from Ref. 12).

Let us first look at the local DOS and its *local* spin polarization. In the Mn ML, the unoccupied *d* states are almost entirely of minority spin type. In the V ML, the states be-

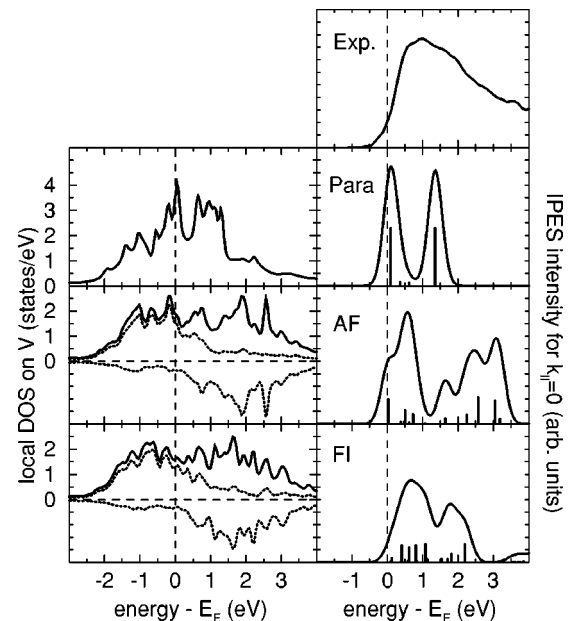


FIG. 7. Same as Fig. 6 for V/Ag(111). For the FI state, a weighted average of the two inequivalent sites is shown.

tween the Fermi level (E_F) and E_F+1 eV are only weakly spin polarized, but the states above E_F+1 eV are mostly of minority-spin type. This is valid for all obtained magnetic solutions and confirms the interpretation given in the experimental paper,¹² namely that the IPES states are of minority-spin type, which, however, must be understood as local spin polarization.

The experimental IPES line shape of the Mn ML shows two peaks at 0.9 and 1.8 eV above E_F . In Ref. 12, the two-peak structure was interpreted as being due to a crystal-field splitting. This could not clearly be proven, however, because *ab initio* results were only available for Mn impurities in Ag and ferromagnetically ordered Mn ML's on Ag(100). In our calculated IPES spectrum for the FO state we indeed observe a clear crystal-field splitting. The high-energy peak mainly comes from (minority-spin) d_{yz} and d_{zx} orbitals, which correspond to the irreducible representation E_1 in the D_{6h} point group of the triangular ML.²⁶ The low-energy peak mainly comes from (minority-spin) $d_{x^2-y^2}$ and d_{xy} orbitals (E_2). [The states of $d_{3z^2-r^2}$ character (A_1) lead to broad features below E_F .] For all other magnetic orders, the crystal-field splitting is considerably ‘‘smeared out’’ because of the lower symmetry of the magnetic superstructure. Note that the peak positions in the FO spectrum, 0.7 and 1.7 eV, agree remarkably well with the experimental spectrum. If a finite background is subtracted from the latter, the intensity of the two peaks becomes approximately equal (see Ref. 12), which is also in agreement with the FO line shape. The line shape of the AF state agrees much less with the experimental spectrum.

In the C state, which has lowest energy among the considered states, line shape and splitting are in quite good agreement with experiment, but the peak positions are by 0.5 eV too low. We shall suggest two possible explanations for this discrepancy. In low-dimensional TM systems, intrasite d - d electron correlation is increased compared to the bulk TM's. For a Mn-Cu surface alloy on Cu(100), this was shown experimentally by Rader *et al.*²⁷ We expect it also to be true for a Mn ML on Ag(111). Such correlations increase the splitting between occupied and unoccupied parts of the d band. The fact that electronic structure methods using the LDA (or the GGA) cannot reproduce these correlation effects correctly, might explain why the peaks of the calculated IPES are too low in energy. Another possible explanation are structural imperfections of the samples. In particular, interdiffusion could have occurred at the Mn-Ag interface. This would lead to a decrease of the Mn-Mn coordination, a reduced d -band dispersion and thus to a more atomlike line shape. Furthermore, this might change the order of stability between the different magnetic states, since the energy differences are very small in Mn/Ag(111), and the magnetic coupling strengths $J_{1,2}$ are very sensitive to structural changes [as can be seen from a comparison with Mn/Cu(111) where the NN Mn-Mn distance is 12% smaller].

The experimental IPES line shape of the V ML has very little structure. It mainly consists of one big asymmetric hump between 0.5 and 3 eV above E_F . A crystal-field splitting is clearly visible in the calculated spectra for the paramagnetic state (‘‘Para’’) and the FO state (not shown), but was not observed experimentally. While none of the calculated line shapes reproduces the experimental one satisfacto-

rily, the spectrum of the FI state comes closest to it. As we found the FI state to be lowest in energy, this is in agreement with our calculations.

V. CONCLUSIONS

In summary, we have studied the magnetic structure of $3d$ TM ML's on Cu(111) and Ag(111) by means of *ab initio* calculations in various collinear spin structures. The choice of the spin structures was motivated by known results on localized spin models, which were also used for a simple interpretation of the results and their limitations (especially with respect to noncollinear spin order). We systematically compared our results with those for ML's on Cu(100) or Ag(100), in order to reveal the specific properties of $3d$ TM's on a triangular lattice. In the light of this comparison the most interesting results are the following. (i) The Ni ML's are nonmagnetic both on Cu(111) and on Ag(111). (ii) In the Mn ML's the NNN exchange coupling is as large or even larger than the NN coupling. (iii) For Mn/Ag(111) the NN coupling is weakly ferromagnetic which leads to a complex two-rows-by-two-rows antiferromagnetic structure. (iv) For the ML's on Cu(111), the AF-FO energy difference is considerably decreased as compared to ML's on Cu(100), which is due to the frustration of the NN antiferromagnetic coupling on the triangular lattice. The effect is largest for Cr/Cu(111) which comes close to the nonmagnetic transition.

For V/Ag(111) and Mn/Ag(111) we calculated the IPES for $k_{||}=0$ and compared them with available experimental results. The calculated spectra for the magnetic state of lowest energy agree reasonably well with the experimental ones.

We have discussed the problem of noncollinear magnetic order in the framework of the Heisenberg model, from which we expect V/Ag(111), Cr/Ag(111) and probably Cr/Cu(111) to have ground states with 120° magnetic order. However, the Heisenberg model provides only a very crude description of the magnetism of TM's. A very interesting extension of this work would be to check these conjectures by *ab initio* calculations for noncollinear magnetism (see, for example, Ref. 28).

ACKNOWLEDGMENTS

The authors thank C. Demangeat, C. Lacroix, and J.-C. Parlebas for stimulating discussions and careful reading of the manuscript.

APPENDIX: ESTIMATION OF THE INTERLAYER DISTANCE AT THE INTERFACE

For the TM-Cu interface, we took the same interlayer spacing as that between two Cu(111) layers since the bulk atomic volumes of the $3d$ -TM's from V to Ni are all approximately the same as that of Cu. (The Wigner-Seitz radii differ from that of Cu by between -3% and $+5\%$.) As mentioned in the Introduction, in the case of thin Fe films on Cu(111), the absence of relaxation was also observed experimentally.³ The atomic volume of fcc Ag, however, is considerably larger than that of the $3d$ elements. (The Wigner-Seitz radius is larger by $7-16\%$.) Therefore for the TM-Ag interfacial distance we took into account an inward

relaxation of 15%, i.e., $d(\text{TM-Ag}) = d_0(\text{Ag}) - 15\%$. This value was determined as follows: for the Wigner-Seitz radii of the TM atoms we took the same value as in the TM/Cu(111) calculations (i.e., that of fcc Cu). $d/(\text{TM-Ag})$ is

then naturally chosen as the mean value between $d_0/(\text{Ag})$ and the (111) interlayer distance of a (hypothetical) pseudomorphically grown fcc Cu film that is vertically distorted such that the Cu atomic volume is kept constant.

-
- ¹P. Schieffer, C. Krembel, M. C. Hanf, and G. Gewinner, *Surf. Sci.* **400**, 95 (1998).
- ²M. Wuttig, Y. Gauthier, and S. Blügel, *Phys. Rev. Lett.* **23**, 3619 (1993).
- ³J. Shen *et al.*, *Phys. Rev. Lett.* **80**, 1980 (1998).
- ⁴S. Blügel and P. H. Dederichs, *Europhys. Lett.* **9**, 597 (1989).
- ⁵S. Blügel, *Appl. Phys. A: Mater. Sci. Process.* **63**, 595 (1996).
- ⁶J. C. Boettger, *Phys. Rev. B* **48**, 10 247 (1993).
- ⁷L. Zhong, R. Wu, A. J. Freeman, and G. B. Olson, *J. Appl. Phys.* **81**, 4479 (1997).
- ⁸J. Redinger, S. Blügel, and R. Podloucky, *Phys. Rev. B* **51**, 13 852 (1995).
- ⁹P. Krüger, A. Rakotomahevitra, J. C. Parlebas, and C. Demangeat, *Phys. Rev. B* **57**, 5276 (1998).
- ¹⁰Y. Tanaka and N. Uryû, *J. Phys. Soc. Jpn.* **39**, 825 (1975).
- ¹¹D. H. Lee, J. D. Joannopoulos, J. W. Nagele, and D. P. Landau, *Phys. Rev. Lett.* **52**, 433 (1984).
- ¹²W. Drube and F. J. Himpsel, *Phys. Rev. B* **35**, 4131 (1987).
- ¹³O. K. Andersen and O. Jepsen, *Phys. Rev. Lett.* **53**, 2571 (1984); O. K. Andersen, Z. Pawłowska, and O. Jepsen, *Phys. Rev. B* **34**, 5253 (1986). The standard TB-LMTO-ASA code (version 47) developed by O. K. Andersen *et al.* at M.P.I. Stuttgart, Germany, was used.
- ¹⁴H. L. Skriver and N. M. Rosengaard, *Phys. Rev. B* **43**, 9538 (1991).
- ¹⁵D. C. Langreth and M. J. Mehl, *Phys. Rev. Lett.* **47**, 446 (1981); C. D. Hu and D. C. Langreth, *Phys. Scr.* **32**, 391 (1985).
- ¹⁶M. Methfessel, C. O. Rodriguez, and O. K. Andersen, *Phys. Rev. B* **40**, 2009 (1989).
- ¹⁷B. Weimert, J. Noffke, and L. Fritsche, *Surf. Sci.* **289**, 397 (1993).
- ¹⁸M. Taguchi, C. Demangeat, J. C. Parlebas, and P. Krüger, *Computat. Mater. Sci.* (to be published).
- ¹⁹P. E. Blöchl, O. Jepsen, and O. K. Andersen, *Phys. Rev. B* **49**, 16 223 (1994).
- ²⁰R. Ballou, C. Lacroix, and M. D. Nunez Regueiro, *Phys. Rev. Lett.* **66**, 1910 (1991).
- ²¹C. Pinettes and C. Lacroix, *Solid State Commun.* **85**, 565 (1993).
- ²²U. von Barth and L. Hedin, *J. Phys. C* **5**, 1629 (1972).
- ²³J. Tersoff and L. M. Falikov, *Phys. Rev. B* **26**, 6186 (1982).
- ²⁴In the spin structure C of the free (111) ML two sites in the magnetic unit cell that have the same spin orientation are equivalent due to a C_2 point symmetry. Since the C_{3v} point symmetry of the fcc (111) surface is incompatible with C_2 , the C_2 symmetry is broken in the adsorbed ML. Consequently, the magnetic moments differ slightly between the two up (or down) spins; we actually obtained the values ± 3.66 and $\pm 3.64\mu_B$. However, these variations are smaller than the numerical error and therefore not significant.
- ²⁵M. Kaburagi and J. Kanamori, *J. Phys. Soc. Jpn.* **44**, 718 (1978).
- ²⁶In fact, \mathcal{D}_6 is the point group of the *free* monolayer; upon adsorption on a fcc (111) surface the point symmetry is lowered to C_{3v} . However, this perturbation seems to be too weak to affect the crystal field significantly.
- ²⁷O. Rader *et al.*, *Europhys. Lett.* **39**, 429 (1997).
- ²⁸J. Sticht, K.-H. Höck, and J. Kübler, *J. Phys.: Condens. Matter* **1**, 8155 (1989).